In Vivo MR Imaging of Magnetically Labeled Mesenchymal Stem Cells in a Rat Model of Renal Ischemia

Sung Il Jung, MD[1]
Seung Hyup Kim, MD[2]
Hyo-Cheol Kim, MD[3]
Kyu Ri Son, MD[4]
Se Young Chung, BSc[3]
Woo Kyung Moon, MD[3]
Hoe Suk Kim, PhD[3]
Jong-Sun Choi, MD[5]
Min Hoan Moon, MD[6]
Chang-Kyu Sung, MD[4]

Index terms:
Mesenchymal stem cell
Superparamagnetic iron oxide, MR
Kidney, ischemia

DOI:10.3348/kjr.2009.10.3.277

Korean J Radiol 2009;10:277-284
Received July 9, 2008; accepted after revision December 8, 2008.

[1]Department of Radiology, Konkuk University Medical Center, Research Institute of Medical Science, Konkuk University School of Medicine, Seoul 143-729, Korea; [2]Department of Radiology, Seoul National University College of Medicine; The Institute of Radiation Medicine, Kidney Research Institute; Seoul National University Medical Research Center, Seoul 110-744, Korea; [3]Department of Radiology, Seoul National University Hospital, Seoul National University College of Medicine, Seoul 110-744, Korea; [4]Department of Radiology, Seoul National University Boramae Hospital, Seoul 156-707, Korea; [5]Department of Pathology, Dongguk University International Hospital, Dongguk University College of Medicine, Goyang 410-773, Korea; [6]Department of Radiology, Cheil General Hospital & Women's Healthcare Center, Kwandong University School of Medicine, Seoul 100-380, Korea.

Address reprint requests to:
Sung Il Jung, MD, Department of Radiology, Konkuk University Medical Center, Research Institute of Medical Science, Konkuk University School of Medicine, 4-12 Hwayang-dong, Gwangjin-gu, Seoul 143-729, Korea.
Tel. (822) 2030-5543
Fax. (822) 2030-5549
e-mail: radsijung@kuh.ac.kr

Objective: This study was designed to evaluate *in vivo* MR imaging for the depiction of intraarterially injected superparamagnetic iron oxide (SPIO)-labeled mesenchymal stem cells (MSCs) in an experimental rat model of renal ischemia.

Materials and Methods: Left renal ischemia was induced in 12 male Sprague-Dawley rats by use of the catheter lodging method. *In vivo* MR signal intensity variations depicted on T2*-weighted sequences were evaluated in both the left and right kidneys prior to injection (n = 2), two hours (n = 4), 15 hours (n = 2), 30 hours (n = 2) and 72 hours (n = 2) after injection of SPIO-labeled MSCs in both kidneys. Signal intensity variations were correlated with the number of Prussian blue stain-positive cells as visualized in histological specimens.

Results: In an *in vivo* study, it was determined that there was a significant difference in signal intensity variation for both the left and right cortex (40.8 $\pm$ 4.12 and 26.4 $\pm$ 7.92, respectively) and for both the left and right medulla (23.2 $\pm$ 3.32 and 15.2 $\pm$ 3.31, respectively) until two hours after injection ($p < 0.05$). In addition, signal intensity variation in the left renal cortex was well correlated with the number of Prussian blue stain-positive cells per high power field ($r = 0.98$, $p < 0.05$).

Conclusion: Intraarterial injected SPIO-labeled MSCs in an experimental rat model of renal ischemia can be detected with the use of *in vivo* MR imaging immediately after injection.

Renal ischemia is the most common injury affecting renal tubular function and is responsible for the majority of cases of acute renal failure in hospital settings (1). This form of renal injury causes necrosis of both the proximal tubule and the thick ascending limb, so called acute tubular necrosis (ATN) (2). Following ischemic injury, tubular cells have been found to undergo necrosis, apoptosis, detachment or dedifferentiation, and such dysfunction and loss of tubular cells play a central role in the process underlying renal failure (1, 3). However, the exact pathogenic mechanism of human renal ischemia is still unknown. In addition, there are currently no therapeutic drugs approved by the United States Food and Drug Administration (FDA) for the prevention or treatment of renal ischemic injury (1, 4).

In the past several years, extensive research has been focused on stem cell therapy to create new functional components or to express tissue specific proteins in damaged organs such as the heart, liver, brain, muscle and vascular endothelium (5–7). An experimental study of stem cell therapy of renal disease has shown that adult bone derived cells can contribute to renal remodeling (8). Furthermore, bone marrow derived hematopoietic stem cells can also take part in the regeneration of the renal tubular epithelium after ischemia-reperfusion as demonstrated in mice (9). Central to

the future success of these cell therapies is to evaluate the ability of cells to migrate and engraft to target organs.

The use of magnetic resonance (MR) imaging would be well suited to evaluate the ability of cells to migrate and engraft to target organs, as MR imaging can provide a detailed representation of target organs with excellent soft tissue contrast and with the use of specialized contrast agents. Paramagnetic or modified dextran-coated superparamagnetic iron oxide (SPIO) contrast agents have been used to label cells, allowing the researcher to monitor cellular migration using MR imaging (10–13). However, few studies have addressed the feasibility of the use of *in vivo* MR imaging of cell therapies in models of renal ischemia (14, 15). The aim of the present study is to assess *in vivo* MR imaging with the use of a conventional 3-Tesla MR imaging unit for the depiction of SPIO-labeled mesenchymal stem cells (MSCs) in a rat model of renal ischemia following intraarterial injection.

MATERIALS AND METHODS

Cell Culture and Labeling

Human MSCs (Bio-Whittaker, Walkersville, MD) were grown in mesenchymal stem cell basal medium (MSCBM, Bio-Whittaker) at 37℃ and in a 95% air, 5% CO2 atmosphere. Cells were maintained by replacement of the growth media every four days. Human MSCs were co-cultured in MSCBM containing FDA-approved SPIO particles (Feridex; Berlex, Wayne, NJ). The iron concentrations of the SPIO preparations were 25, 50, 100 and 125 μg/ml.

Poly-L-Lysine (PLL) (Sigma-Aldrich, St. Louis, MO) was used as a transfection agent (TA). PLL coats the SPIO through an electrostatic interaction and binds to the cell membrane while inducing membrane bending; subsequently, SPIO is endocytosed (16). PLL was mixed with SPIO for 60 minutes in mesenchymal stem cell culture medium at room temperature with the use of a rotating shaker. The concentration of the TA was 0.75 μg/ml for each of the SPIO concentrations tested (10). After an incubation period of three days, cells were washed twice with phosphate buffered saline (PBS) to remove excess contrast agent. For Prussian blue staining, cells were fixed for 15 minutes with 4% paraformaldehyde, washed twice with distilled water, and were incubated for 30 minutes with a mixing solution of 0.5% potassium ferrocyanide (Pearl's reagent) and 0.5% HCl, after which the cells were subsequently washed twice with PBS and counterstained with eosin. Labeling efficiency was assessed by determination of the percentage of Prussian blue stain-positive cells following labeling with SPIO at 25, 50, 100 and 125 μg/ml.

The intracellular iron content was quantified after cell labeling by the use of an iron-binding assay. Briefly, cells were incubated with increasing concentrations of SPIO for 24 hours in the presence of PLL (0.75 μg/ml). Cells were then washed with culture medium and were then washed three times with PBS, resuspended in 6 N HCl and were incubated at 70℃ for 30 minutes. The iron content of labeled cells was determined by use of a total iron reagent set (Pointe Scientific, Canton, MI). With knowledge of the iron content and the number of cells per sample, the average iron content per cell was calculated (mean ± standard deviation). The iron content of non-labeled cells was also measured to obtain a control value.

The presence of SPIO particles was evaluated within cells by the use of electron microscopy. Human MSCs were fixed in a 1% dilution of 6% tannic acid and 25% glutaraldehyde (Sigma-Aldrich). Fixed cells were embedded on Thermanox plates (Nunc, Langenselbold, Germany) and gelatin capsules filled with Epon, followed by polymerization for 48 hours at 60℃. Electron microscopy (JEM-100CX, JEOL, Tokyo, Japan) was performed. Serial analysis was performed by using magnifications ranging from ×4,400 to ×85,000. An experienced board-certified pathologist performed visual analysis with the use of electron microscopy.

Assessment of Viability and Proliferation

For assessment of toxicity and proliferation of SPIO-labeled cells, human MSCs were evaluated with trypan blue staining to verify membrane integrity. Cells were labeled at SPIO concentrations of 25, 50, 100 and 125 μg/ml in 60 mm plates. After 1, 3 and 5 days, cells were washed three times with PBS, trypsinized and were collected in Eppendorf tubes. Cells were counted three times with a hematocytometer to measure both viability and proliferation.

Animal Models

All animal work was conducted in accordance with the guidelines provided by the Institutional Animal Control and Utilization Committee. For all manipulations, rats were anesthetized with a 0.6–0.8 cc intramuscular injection of 35–50 mg/kg ketamine hydrochloride (Yuhan Yanghang, Seoul, Korea) and 5–10 mg/kg 2% xylazine hydrochloride (Bayer Korea, Seoul, Korea).

Male Sprague-Dawley rats (n = 12) (weight range, 320–400 g; age range, 10–13 weeks) were first anesthetized and a 1.9 Fr microcatheter (Prowler-14, Cordis, Miami Lakes, FL) was subsequently inserted into the mid common carotid artery that had been previously exposed with a paramedian incision of approximately 2 cm in the rat neck.

Next, the microcatheter was lodged in the proximal left renal artery for 40 minutes through the carotid artery and thoracic aorta. Reflow was confirmed by the use of left renal angiography with contrast media (3 cc; Pamiray, Dongkook Pharmaceutical, Seoul, Korea) (Fig. 1). The aforementioned procedure provided the rat models with an ischemic and normal kidney on the left and right side, respectively.

For injection preparation, human MSCs (Bio-Whittaker) were labeled with 0.01% TA and 125 μg/ml SPIO for 48 hours. Next, cells were washed three times with PBS, trypsinized, washed twice after centrifugation at 300 ×g for five minutes, and were counted. Cells were suspended at 2 × 106/0.5 cc in PBS and were injected into both renal arteries after selective renal angiography by the use of a transcarotid approach. Rats were imaged immediately after ischemia was induced prior to injection as a baseline image (n = 2), and then two hours (n = 4), 15 hours (n = 2), 30 hours (n = 2) and 72 hours (n = 2) after the injection. Rats were sacrificed immediately after MR imaging and both kidneys were harvested for histological studies.

In order to compare the degree and extent of tubular injury obtained with the method in the present study as compared with the use of previously established models using renal artery clamping, we evaluated tubular injury in a histological specimen of a sacrificed ischemic kidney using previously reported histological criteria after use of the catheter lodging method (n = 2) and surgical clamping (n = 2) (17). After we stained three axial sections of each fixed kidney with Hematoxylin and Eosin, the degree of tubular injury in random cortex and medulla fields was scored with nine squares for each kidney with a high-power field (HPF), and scores were compared for specimens obtained by use of the catheter lodging method and surgical clamping. A score for each tubular injury was assigned as follows. Score 0 = normal histology; score 1 = tubular cell swelling, with loss of the brush border, nuclear condensation (apoptosis), up to one-third of the section that showed nuclear loss (necrosis); score 2 = the same as for score 1, except for greater than one-third and less than two-thirds of nuclear loss per section; score 3 = greater than two-thirds of the section showed nuclear loss (necrosis).

MR Imaging

All MR imaging was performed with a 3-Tesla clinical unit (Signa Excite; GE Healthcare, Milwaukee, WI) with an 8-channel head coil. T2* weighted gradient echo sequences (repetition time msec/echo time msec, 400/15; flip angle, 15°) were used to enhance the T2* effects of the SPIO particles. The following image parameters were used: field of view, 80×80 mm; matrix size, 256×160; section thickness, 3 mm; number of excitation, 3; total acquisition time, 3.40 minutes. Both kidneys were imaged in the axial plane.

Changes in signal intensity (SI) were characterized by use of region of interest (ROI) analysis on a well-centered slice with an area of 1 mm^2. A minimum of 15 pixels was required per region as displayed on a picture archiving and communication system (PACS) workstation (Maroview; Marotech, Seoul, Korea). The ROI was selected for the renal cortex and medulla, and was placed to avoid susceptibility effects arising from air-tissue interfaces in the bowels. The value of the ROI was determined as the mean ± standard deviation after an estimated three times in the upper pole, mid region and lower pole of each cortex or medulla per one kidney, and was normalized to that of back muscle (18, 19). SI changes in each rat were calculated according to the use of the following formula: (SI [pre] − SI [post])/SI (pre)×100; SI (pre) and SI (post) are the normalized SI values as compared to back muscle before and after labeled cell injection.

Histological Analysis

Rat kidney tissue blocks were fixed in 4% paraformaldehyde and were processed for paraffin embedding. Microsections (4 μm) were prepared with a microtome and were used for Prussian blue staining to detect labeled iron particles in the cells. An experienced board-certified pathologist calculated the number of Prussian blue stain-positive cells per HPF in each group. Prussian blue stain-positive cells were counted in at least three HPFs per section and a minimum of six sections of each kidney were examined.

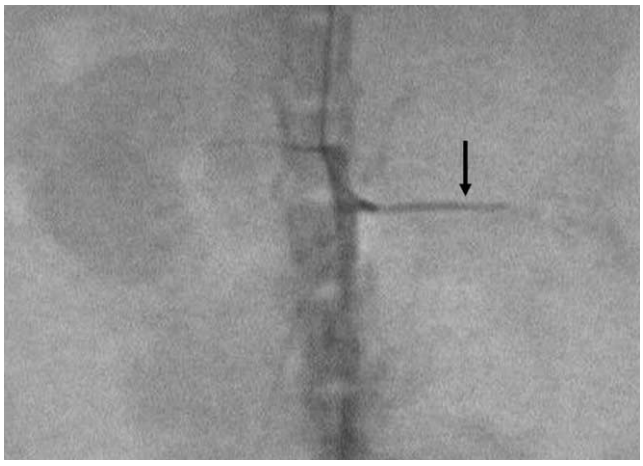

Fig. 1. Left renal angiography after lodging in left renal artery with microcatheter. Left renal angiography shows sluggish left renal flow (arrow) after lodging for 40 minutes.

Statistical Analysis

The Mann-Whitney test and Spearman's rank correlation were used to assess the variation between groups. A p value < 0.05 was considered as statistically significant.

RESULTS

In Vitro Studies

For Prussian blue staining of human MSCs incubated with varying concentrations of SPIO, numerous intracytoplasmic iron particles were observed in the MSCs with Prussian blue staining. In cells incubated with 25, 50, 100 and 125 μg/ml SPIO for one day, there were 97 $\pm$ 2.3, 97 $\pm$ 2.7, 98 $\pm$ 0.5 and 99 $\pm$ 1.0 Prussian blue stain-positive cells per 100 cells, respectively. There was no significant difference among the labeled cells according to concentration of SPIO ($p > 0.05$). Electron microscopy demonstrated that SPIO particles were present in endosomal vesicles (Fig. 2).

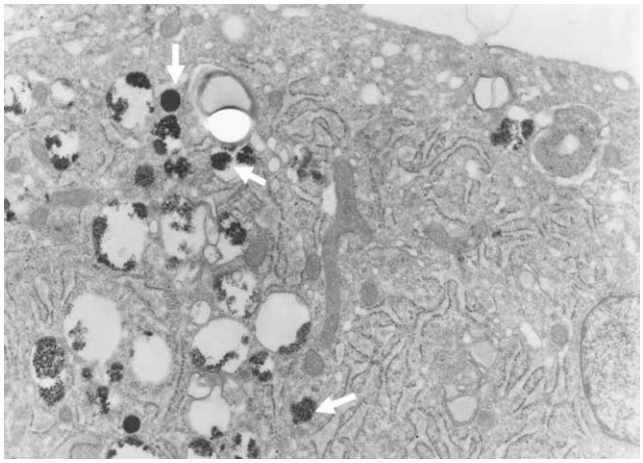

Fig. 2. Electron micrograph of superparamagnetic iron oxide labeled mesenchymal stem cells (original magnification, $\times$4,800). There are multiple endosomal vesicles containing superparamagnetic iron oxide particles (arrows) seen in cytoplasm of mesenchymal stem cells.

The mean intracellular iron content at 25, 50, 100 and 125 μg/ml SPIO was 257 $\pm$ 8.7, 240 $\pm$ 12.6, 322 $\pm$ 11.3 and 255 $\pm$ 5.5 pg/cell in comparison to 0.02 $\pm$ 0.04 pg/cell in the non-labeled control group. There was no significant difference between the mean intracellular iron content of labeled cells.

Five days after the initiation of SPIO labeling, no statistically significant decrease in the number of cells ($p > 0.05$) or cell viability ($p > 0.05$) was observed for labeled and control cells (non-labeled MSCs) at SPIO concentrations up to 125 μg/ml (Fig. 3).

In Vivo Animal Studies

Following intraarterial injection of labeled MSCs in both the ischemic and control kidneys, a decrease in SI, which was produced by susceptibility effects of SPIO, was observed in the renal cortex and medulla on T2*-weighted images (Fig. 4). The change in SI in the renal cortex and medulla on T2*-weighted images peaked at two hours after injection and subsequently declined (Fig. 5). Changes in SI in the renal cortex between the ischemic and control kidney were significantly different at two hours after injection (40.8 $\pm$ 4.12 for the ischemic cortex and 26.4 $\pm$ 7.92 for the control cortex; $p < 0.05$) but was not significantly different at 15, 30, and 72 hours after injection. Similarly for the renal medulla, changes in SI between the

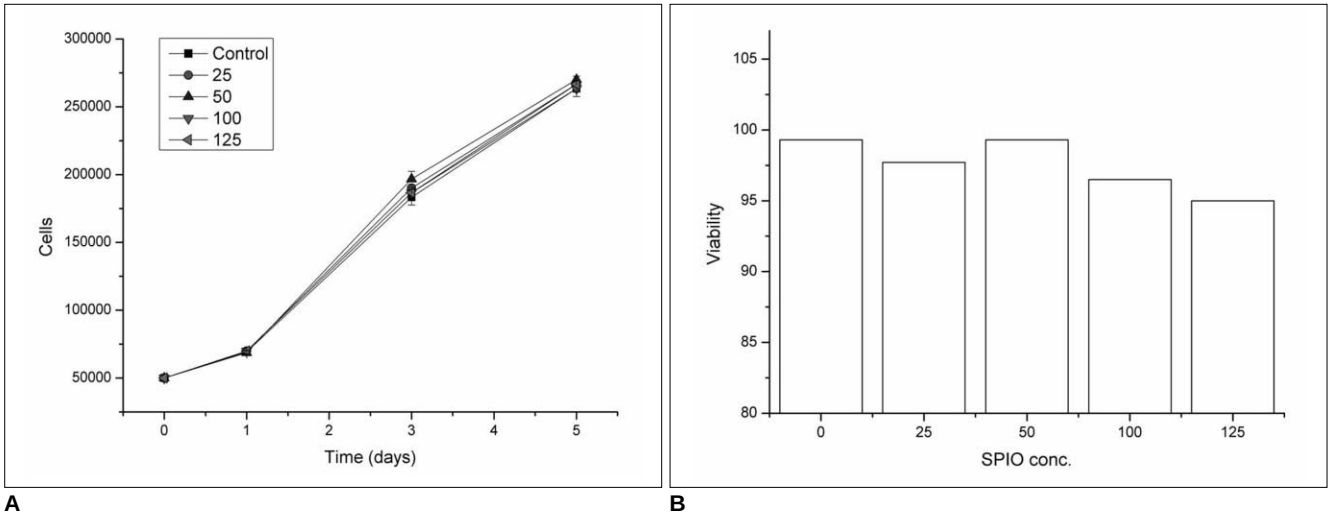

A **B**

Fig. 3. Cell proliferation and viability of superparamagnetic iron oxide labeled mesenchymal stem cells. Any significant difference in number of cells was not observed between control cells and superparamagnetic iron oxide labeled cells for concentrations up to 125 μg/ml for cell proliferation (**A**) and cell viability (**B**). Data are shown as means $\pm$ standard deviation.

ischemic and control kidney were significantly different at two hours after injection (23.2 $\pm$ 3.32 for the ischemic medulla and 15.2 $\pm$ 3.31 for the control medulla; $p <$ 0.05) but not at any time thereafter.

Prussian blue staining was used to identify SPIO particles in the ischemic and control kidney (Fig. 6). The number of Prussian blue stain-positive cells per HPF in the renal cortex and medulla of the ischemic kidney peaked at two

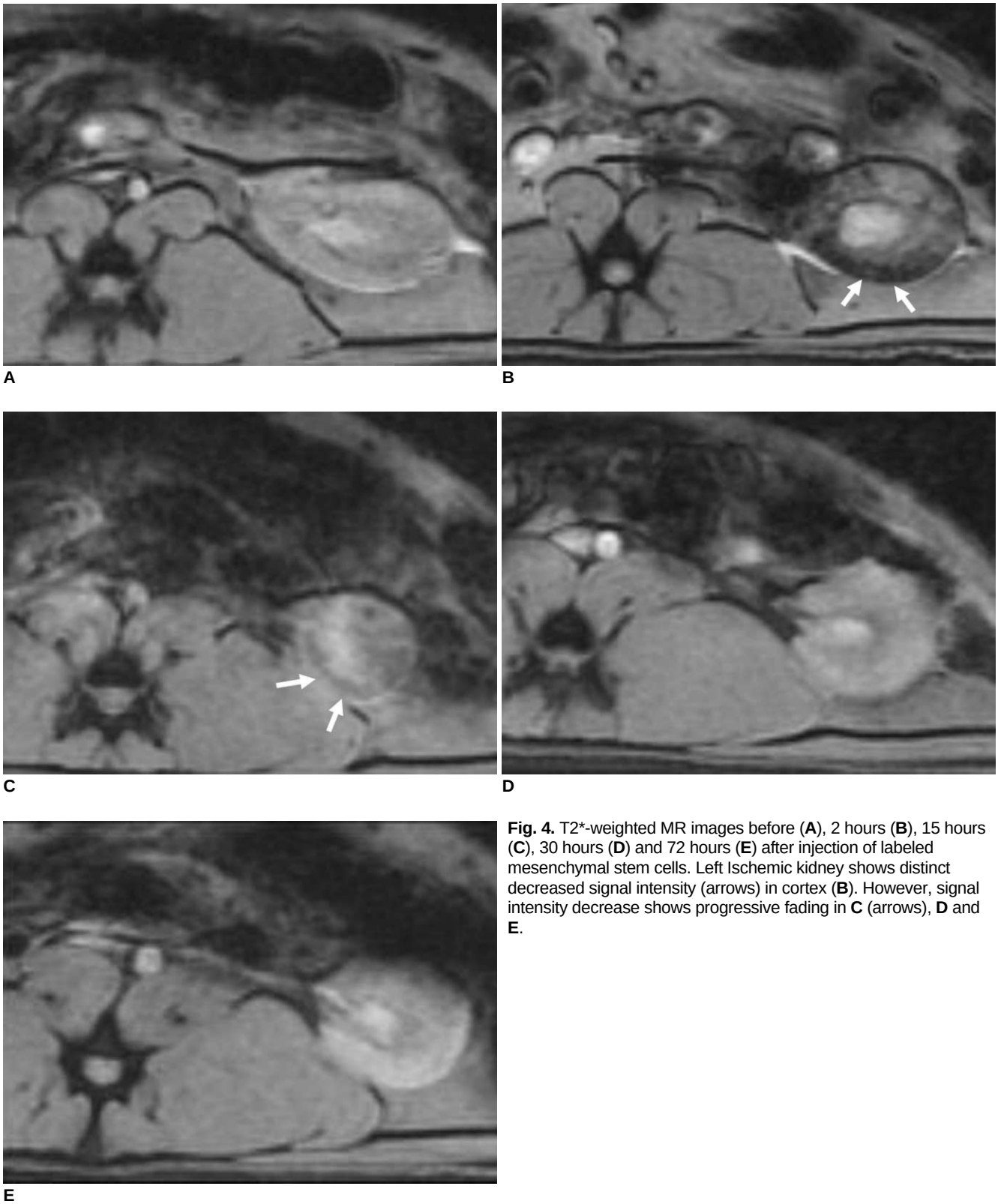

Fig. 4. T2*-weighted MR images before (**A**), 2 hours (**B**), 15 hours (**C**), 30 hours (**D**) and 72 hours (**E**) after injection of labeled mesenchymal stem cells. Left Ischemic kidney shows distinct decreased signal intensity (arrows) in cortex (**B**). However, signal intensity decrease shows progressive fading in **C** (arrows), **D** and **E**.

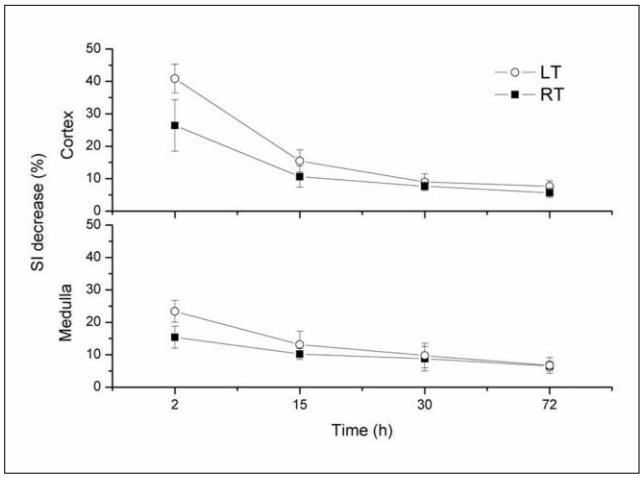

Fig. 5. Time course of signal intensity decrease on T2*-weighted image.
Graph shows that signal intensity change on T2*-weighted image in renal cortex and medulla decreases with time after injection of labeled mesenchymal stem cells. Difference for signal intensity change was prominent at two hours in renal cortex and medulla for ischemic kidney (LT) and control kidney (RT). Data are shown as means ± standard deviation.

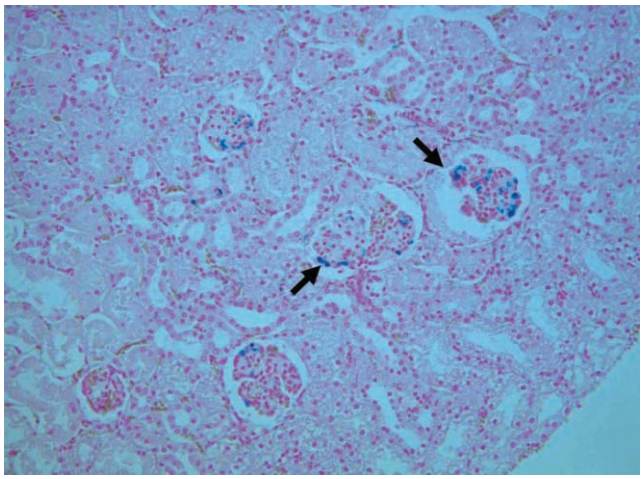

Fig. 6. Micrograph of histological specimen of ischemic kidney obtained at two hours after superparamagnetic iron oxide labeled mesenchymal stem cells injection (original magnification, ×200). Arrows indicate Prussian blue stain-positive particles in glomeruli and tubules of renal cortex.

hours after injection and subsequently declined (Fig. 7). There were significantly more Prussian blue stain-positive particles per HPF in the cortex and medulla ischemic kidneys than in the control kidneys. The number of Prussian blue stain-positive particles per HPF peaked at two hours after injection (25.7 ± 5.31 for the ischemic cortex and 11.2 ± 7.36 for the control cortex; $p < 0.05$; 6.7 ± 3.13 for the ischemic medulla and 2.2 ± 1.17 for the control medulla; $p < 0.05$). The number of Prussian blue stain-positive cells per HPF in the cortex of the

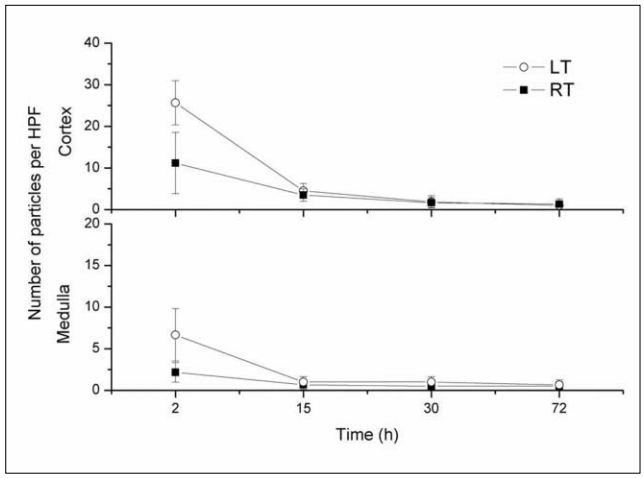

Fig. 7. Time course of number of Prussian blue staining-positive cells per high-power field. Graph shows number of Prussian blue stain-positive cells in renal cortex and medulla after labeled mesenchymal stem cells injection as function of time. At two hours after injection, sharp decrease in number of cells is observed in renal cortex and medulla of ischemic kidney (LT). Gradual decrease in number of particles is observed in renal cortex and medulla of control kidney (RT). Data are shown as means ± standard deviation.

ischemic kidney was positively correlated with a decrease in SI ($r = 0.98$, $p < 0.05$). However, the number of Prussian blue stain-positive cells per HPF in the medulla of ischemic kidney was not significantly correlated with a decrease in SI ($r = 0.94$, $p > 0.05$).

For the comparison between specimens obtained with use of the catheter lodging method and specimens obtained with use of surgical clamping, we did not find any significant differences with respect to the score of injury between the use of the catheter lodging method (2.1 ± 0.68) and surgical clamping (2.3 ± 0.84) ($p > 0.05$).

DISCUSSION

The results of our study have demonstrated that human MSCs could be successfully labeled *in vitro* with commercially available SPIO particles and a transfection agent. Moreover, we have demonstrated that due to the susceptibility effect, SPIO labeled MSCs could be detected *in vivo* by the use of a clinically available 3-Tesla MR unit after intraarterial injection in a rat model of renal ischemia.

Results obtained with the use of *in vitro* labeled human MSCs in our study generally agreed with findings of previous studies that have demonstrated the usefulness of iron oxide particles to label MSCs (10, 20, 21). It is important that labeled MSCs maintain the ability to differentiate in a given concentration of SPIO, as labeled MSCs used in cell therapy are expected to differentiate in order to regenerate damaged tissues. Therefore, conservation of

viability and proliferation following SPIO labeling is essential. Our results indicate that there was no significant difference in cell viability and proliferation between control cells and cells labeled with up to 125 μg/ml SPIO; this concentration of SPIO was determined to exhibit the highest SI change for cells in an *in vivo* study.

The rat ischemic model was based on the use of the catheter lodging method in the renal artery for 40 minutes with a transcarotid approach. We chose this method primarily as it is a less invasive technique than the use of renal artery clamping after transperitoneal incision, which results in a reduction of experimental animal mortality. In addition, the technique is a more sophisticated method to confirm the presence of reflow and spasm of the renal artery of the ischemic kidney. There were no significant differences between the use of the catheter lodging method and the surgical clamping method with respect to the extent of injury with more than a score of 1. However, we have speculated that the catheter lodging method could not produce global high-grade tubular injury more frequently than the surgical clamping method due to the difficulty of causing a tight occlusion.

In most reports that have described MR imaging of magnetically labeled MSCs, local implantation has been used as the route for cell grafting into the rat brain and spinal cord (22, 23). Such an invasive approach is not suitable for the kidney, where damaged components often have a widespread distribution, and stereotactic methods cannot be applied due to the influence of respiratory motion. Thus, we used an intraarterial route for cell grafting, as a large number of cells could be directly delivered to the target organ.

The histological data obtained in the present study showed that Prussian blue stain-positive cells were found mainly within the renal cortex of the ischemic kidney at two hours after injection. This finding may be due to cells that were mechanically trapped in the damaged glomerular tuft or was due to active recruitment to the acute injury site. However, it was likely that mechanical trapping was the dominant factor based on the immediate presence of Prussian blue stain-positive cells and rapid fading in the renal cortex from 15 hours after injection. Regardless of whether the predominant presence of Prussian blue stain-positive cells in the ischemic cortex was due to passive effects or local trophic effects, a decrease in the number of Prussian blue stain-positive cells was observed in the ischemic renal cortex. In addition, the decrease in the number of stained cells was well correlated with a change in SI as seen on a T2*-weighted MR image. Eventually, the difference in SI between the ischemic and normal cortex was not significant at 15, 30 and 72 hours after injection. This finding suggested that the SPIO labeled cells were predominantly detected only in the ischemic cortex immediately after injection; thereafter, only a small number of SPIO labeled cells were retained in both the ischemic and normal cortex, presumably by the same mechanism.

In the ischemic renal medulla, we did observe a gradual decrease in the number of Prussian blue stain-positive cells; however, this pattern was not significantly correlated with a change in SI as seen on a T2*-weighted MR image. The lack of correlation may have been due to a small number of samples that were insufficient for statistical significance, or was due to the presence of a tubular cast containing hemoglobin or hemorrhage that usually occurs in the medulla of ischemic ATN, which caused a confounding susceptibility effect as seen on a T2*-weighted MR image.

There are some limitations to this study. First, we used only commercially available human MSCs, and not rat MSCs, to facilitate an *in vitro* process as we focused on the validity of MR imaging for the depiction of SPIO-labeled MSCs in renal ischemia rather than to assess recovery of renal function. Second, we did not perform immunohistochemical analysis on human MSCs under the conditions that we tested with the rat model, and therefore could not confirm whether Prussian blue stained positive particles were associated with labeled SPIO in MSCs *in vivo*. Third, the number of animals in this study was not sufficient to reproduce and statistically analyze the current results. Fourth, a study evaluating cell trafficking through intravenous injection, for example, with MR imaging of the spleen, bone marrow and liver, should be conducted to identify the mechanism of targeted cellular homing to damaged components. Finally, we did not perform an intraindividual longitudinal comparison of MR SI variation in rats due to the relatively short survival period after such procedures as catheter lodging and the use of frequent MR scanning.

In conclusion, intraarterial injected SPIO-labeled MSCs in renal ischemia induced in the rat can be depicted with the use of *in vivo* MR imaging immediately after injection.

Acknowledgement

This study was partly supported by a grant from the Seoul Research and Business Development Program 10548 and by a grant (A062260) from the Innovative Research Institute for Cell Therapy, Republic of Korea.

References

1. Thadhani R, Pascual M, Bonventre JV. Acute renal failure. *N Engl J Med* 1996;334:1448-1460
2. Shanley PF, Rosen MD, Brezis M, Silva P, Epstein FH, Rosen S. Topography of focal proximal tubular necrosis after ischemia

with reflow in the rat kidney. *Am J Pathol* 1986;122:462-468
3. Sutton TA, Molitoris BA. Mechanisms of cellular injury in ischemic acute renal failure. *Semin Nephrol* 1998;18:490-497
4. Kelly KJ, Molitoris BA. Acute renal failure in the new millennium: time to consider combination therapy. *Semin Nephrol* 2000;20:4-19
5. Grove JE, Bruscia E, Krause DS. Plasticity of bone marrow-derived stem cells. *Stem Cells* 2004;22:487-500
6. Herzog EL, Chai L, Krause DS. Plasticity of marrow-derived stem cells. *Blood* 2003;102:3483-3493
7. Krause DS. Plasticity of marrow-derived stem cells. *Gene Ther* 2002;9:754-758
8. Gupta S, Verfaillie C, Chmielewski D, Kim Y, Rosenberg ME. A role for extrarenal cells in the regeneration following acute renal failure. *Kidney Int* 2002;62:1285-1290
9. Kale S, Karihaloo A, Clark PR, Kashgarian M, Krause DS, Cantley LG. Bone marrow stem cells contribute to repair of the ischemically injured renal tubule. *J Clin Invest* 2003;112:42-49
10. Frank JA, Miller BR, Arbab AS, Zywicke HA, Jordan EK, Lewis BK, et al. Clinically applicable labeling of mammalian and stem cells by combining superparamagnetic iron oxides and transfection agents. *Radiology* 2003;228:480-487
11. Josephson L, Tung CH, Moore A, Weissleder R. High-efficiency intracellular magnetic labeling with novel superparamagnetic-Tat peptide conjugates. *Bioconjug Chem* 1999;10:186-191
12. Lewin M, Carlesso N, Tung CH, Tang XW, Cory D, Scadden DT, et al. Tat peptide-derivatized magnetic nanoparticles allow in vivo tracking and recovery of progenitor cells. *Nat Biotechnol* 2000;18:410-414
13. Hauger O, Frost EE, van Heeswijk R, Deminière C, Xue R, Delmas Y, et al. MR evaluation of the glomerular homing of magnetically labeled mesenchymal stem cells in a rat model of nephropathy. *Radiology* 2006;238:200-210
14. Bulte JW, Kraitchman DL. Iron oxide MR contrast agents for molecular and cellular imaging. *NMR Biomed* 2004;17:484-499
15. Ittrich H, Lange C, Tögel F, Zander AR, Dahnke H, Westenfelder C, et al. In vivo magnetic resonance imaging of iron oxide-labeled, arterially-injected mesenchymal stem cells in kidneys of rats with acute ischemic kidney injury: detection and monitoring at 3T. *J Magn Reson Imaging* 2007;25:1179-1191
16. Kalish H, Arbab AS, Miller BR, Lewis BK, Zywicke HA, Bulte JW, et al. Combination of transfection agents and magnetic resonance contrast agents for cellular imaging: relationship between relaxivities, electrostatic forces, and chemical composition. *Magn Reson Med* 2003;50:275-282
17. Tögel F, Hu Z, Weiss K, Isaac J, Lange C, Westenfelder C. Administered mesenchymal stem cells protect against ischemic acute renal failure through differentiation-independent mechanisms. *Am J Physiol Renal Physiol* 2005;289:F31-F42
18. Firbank MJ, Coulthard A, Harrison RM, Williams ED. A comparison of two methods for measuring the signal to noise ratio on MR images. *Phys Med Biol* 1999;44:N261-N264
19. Jo SK, Hu X, Kobayashi H, Lizak M, Miyaji T, Koretsky A, et al. Detection of inflammation following renal ischemia by magnetic resonance imaging. *Kidney Int* 2003;64:43-51
20. Bos C, Delmas Y, Desmoulière A, Solanilla A, Hauger O, Grosset C, et al. In vivo MR imaging of intravascularly injected magnetically labeled mesenchymal stem cells in rat kidney and liver. *Radiology* 2004;233:781-789
21. Kraitchman DL, Heldman AW, Atalar E, Amado LC, Martin BJ, Pittenger MF, et al. In vivo magnetic resonance imaging of mesenchymal stem cells in myocardial infarction. *Circulation* 2003;107:2290-2293
22. Bulte JW, Ben-Hur T, Miller BR, Mizrachi-Kol R, Einstein O, Reinhartz E, et al. MR microscopy of magnetically labeled neurospheres transplanted into the Lewis EAE rat brain. *Magn Reson Med* 2003;50:201-205
23. Bulte JW, Douglas T, Witwer B, Zhang SC, Strable E, Lewis BK, et al. Magnetodendrimers allow endosomal magnetic labeling and in vivo tracking of stem cells. *Nat Biotechnol* 2001;19:1141-1147